

A multi-scale methodology to model damage, deformation and ignition of highly-filled energetic materials

G. Vivier^{1,2}, H. Trumel², F. Hild¹

¹*LMT Cachan, ENS Cachan/CNRS/University Paris 6/PRES UniverSud Cachan, France;* ²*CEA Le Ripault, Monts, France;*

E-mail: guillaume.vivier@lmt.ens-cachan.fr

Abstract: Some highly-filled energetic materials exhibit a concrete-like microstructure, and behave accordingly. Under moderate (quasi-static or dynamic) confining pressures, their tendency towards strain localization is inhibited. During deformation, micro-cracking occurs in the largest grains, and frictional sliding induces an apparent elasto-plastic behavior. In the dynamic case, this process also produces strong local heating that may lead to ignition.

The present work aims at modeling this two-fold phenomenology by proposing a thermodynamics-based multi-scale approach. The macroscopic material is seen as a statistical distribution of unit cells containing a (cracked) grain embedded in an elastic mortar-like matrix. A (mesoscopic) unit cell model is first developed under confined shear. Owing to the high volume fraction of filler, care must be taken in the meso to macro transition, i.e., the assembling process.

The resulting model captures the essential trends of the mechanical behavior of the materials under consideration. Its thermodynamic ingredients allow for the derivation of the dissipated power and the heat flux on sliding crack lips, thus providing a useful tool towards predicting ignition.

1-Introduction

Energetic materials are widely used for propulsion, mining and military applications, for which safety issues have to be addressed. During unexpected impacts, even at very low velocities, kinetic energy can be converted to heat through dissipative deformation processes. In general, the macroscopic temperature increase remains modest. At lower scale however, due to the heterogeneous nature of most energetic materials, defect-induced temperature peaks can be recorded. Small scale exothermic events, known as “hot spots” [1], may be triggered and represent the very first processes of unwanted explosions.

The exact nature of hot spots is not known formally yet, but is likely to depend on the microstructure, the nature of the energetic crystals, and on the intensity of the load [2]. The material considered herein is an HMX-based energetic composition, whose concrete-like initial microstructure is illustrated in Fig. 1-a. The energetic

HMX crystal is brittle under lightly confined loading, and yields by twinning otherwise. The material of Fig. 1-a, manufactured by isostatic pressing, contains relatively high densities of trans-granular micro-cracks and twins. The study of recovered samples (see, for example, Ref. [3]) showed that (i) massive twinning is prevented as long as the hydrostatic pressure remains below, say, 200 MPa, and that (ii) the micro-crack density evolution is progressively inhibited as the confining pressure increases. Hence, impacts invoking pressures below 300 MPa should involve closed micro-crack slip as the main deformation process, and micro-crack friction as the main hot spot mechanism (Fig. 1-b).

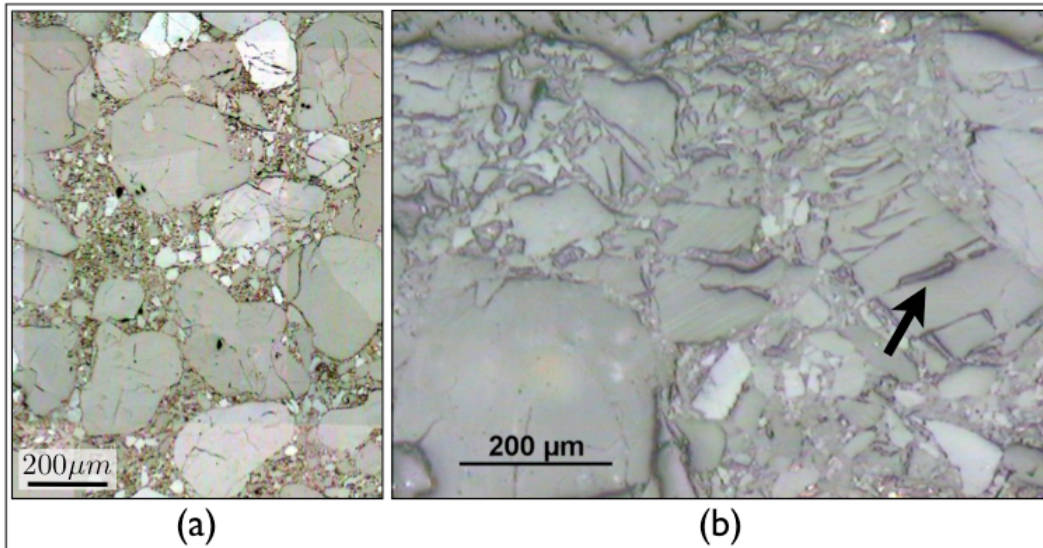


Figure 1: (a) Initial microstructure and after a triaxial compression test (b) - microreaction [4]

2-Scope and methodology

Ignition is the result of the competition between dissipative heating and cooling by thermal conduction. Hot spot ignition is only a necessary condition for macroscopic explosion, because thermal conduction is particularly efficient at the considered scale ($\sim 1\text{-}100\ \mu\text{m}$), and may even induce hot spot extinction. However, this necessary condition can be seen as a useful safety threshold, which can only be assessed by evaluating the intensity of local heating. This is the primary issue of the present study.

Given the space and time scales of a hot spot process, and the complexity of impact events, direct observations are not possible at present, and an indirect “downscale” two-step methodology is promoted here. As shown in Fig. 1-a, the material at stake can be viewed as a distribution of large grains embedded in a continuous matrix. Only large grains contain micro-cracks, the matrix appearing essentially virgin. This picture will be simplified by considering the material as a statistical distribution of elementary cells of the kind depicted in Fig. 2-a. This constitutes the first macro-meso downscale step. Within a representative volume

element, the mesoscopic fields are defined as being uniform on the boundaries of an elementary cell, and allowed to fluctuate from cell to cell.

The second meso-micro downscale step is the scope of the present paper. A generic elementary cell is loaded on its external boundaries by a uniform mesoscopic field. Within the two-dimensional approximation, the mechanical and energetic response of the cell under confined mesoscopic shear is sought. It should be stressed, however, that the volume ratio of grains is of the order of ca. 50%. Uniform boundary traction or linear boundary displacement should thus result in strongly different responses. Consequently, both will be studied in the sequel, the results being considered as bounds in view of the macro-meso downscale step. To derive closed-form relationships, the microscopic fields will obey 1D-like descriptions, hence explaining the form of the elementary cell of Fig. 2-a. The corresponding assumptions will be systematically checked by means of numerical simulations using the ABAQUS Standard finite element code.

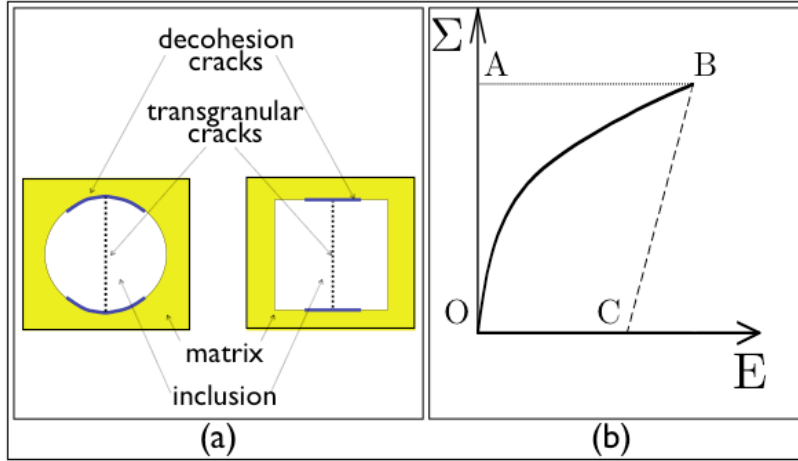


Figure 2: (a) *The individual cell – left: the most realistic geometry – right: the geometry considered for analytical developments.* (b) *Stress-strain curve*

3-General relationships

For both boundary conditions, the following averages stand

$$\Sigma = \frac{1}{V} \int_{\Omega} \sigma dV \quad E = \frac{1}{V} \int_{\partial\Omega} u \times \nu dS = \frac{1}{V} \int_{\Omega} \varepsilon dV + \frac{1}{V} \int_{\Gamma} u \times n dS$$

where Σ and E are the mesoscopic stress and strain tensors, σ , ε and u the microscopic stress in the loaded state B of Fig. 2-b, strain and displacement, Ω the elementary cell of volume V , of external boundary $\partial\Omega$, of external normal ν , Γ denotes collectively the internal crack surfaces of normal n (Fig. 2-a), and the symbol \times is used for the symmetrized tensorial product.

Following Andrieux et al. [5], a (virtual) state C is defined by a purely elastic (virtual) unloading path from point B of Fig. 2-b. State C is characterized by the stress, strain and displacements fields σ^i , ε^i and u^i respectively. Since C is an unloaded state, the field σ^i is self-balanced, and since CB is an elastic path, the superposition principle applies, such that $\sigma = \sigma^i + \sigma^*$ (a), and $\Sigma = \frac{1}{V} \int_{\Omega} \sigma^* dV$.

Then, the mesoscopic strain E is decomposed into $E = E^i + E^*$ (b), where

$$E^i = \frac{1}{V} \int_{\Omega} \varepsilon^i dV + \frac{1}{V} \int_{\Gamma} u^i \times ndS \quad \text{and} \quad E^* = \frac{1}{V} \int_{\Omega} \varepsilon^* dV + \frac{1}{V} \int_{\Gamma} u^* \times ndS$$

In these expressions, $\varepsilon^i = C^{-1} : \sigma^i$ and $\varepsilon^* = C^{-1} : \sigma^*$, where C is the local elastic stiffness tensor. It can be proven that $\psi = W^* + W^i$ (c), where ψ is the (isothermal) free energy, W^i the stored energy, and W^* the elastic energy immediately recoverable upon (virtual) unloading, respectively given by

$$W^i = \frac{1}{V} \int_{\Omega} \sigma^i : C^{-1} : \sigma^i dV \quad \quad W^* = \frac{1}{V} \int_{\Omega} \sigma^* : C^{-1} : \sigma^* dV$$

The knowledge of the free energy allows one to determine the dissipation

$$D = \Sigma : \dot{E}^i - \dot{W}^i$$

and the integral Taylor-Quinney coefficient

$$\beta^{\text{int}} = \frac{W^d}{W^d + W^i}$$

where W^d is the dissipated energy.

4-The cell model

To evaluate the heat flux dissipated by frictional microcracks, the cell is submitted to confined shear, representative of a compressive impact loading. A uniform (mesoscopic) shear stress Σ_{xy} is prescribed on the external boundary (Fig. 3), in addition to normal confining stresses Σ_{xx} and Σ_{yy} . The behavior of the matrix (resp. the inclusion) is considered elastic with a stiffness K_M , Poisson's ratio ν_M and shear modulus C_{xy-M} (resp. K_I , ν_I and C_{xy-I}). The cell is considered as adiabatic.

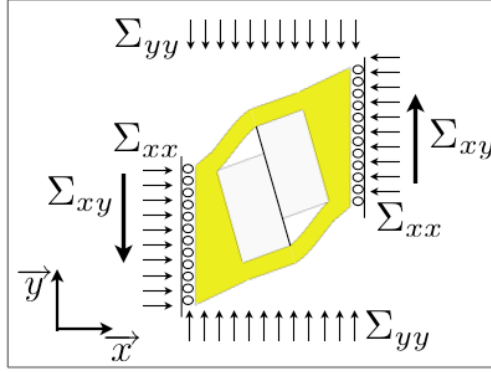


Figure 3: Combined shear and normal loading.

The virtual path (OC)-(CB) previously introduced (Fig. 2b) is used to evaluate the cell response under confined shear. The key point is to choose a method for prescribing the inelastic strain (path (OC)). Since transgranular crack sliding is studied, according to Coulomb's law, and by assuming that the shear stress τ_I is uniform on crack lips, τ_I and Σ_{xx} are related by $\tau_I = fN_I$, where f is the frictional coefficient on cracks lips, and N_I the mean normal stress ($N_I \propto \Sigma_{xx}$). Furthermore, shear stress τ_I^* defined on the inactivated crack of the cell submitted to a load Σ_{xy} (path (CB)) is also assumed to be uniform, and is dependent on Σ_{xy} . The stress partition (a) illustrated in Fig. 4 is invoked to determine the shear stress τ_I^i that needs to be applied on the crack lips to prescribe the inelastic strain and calculate the stored energy. Since τ_I and τ_I^* are uniform, τ_I^i is also uniform, and $\tau_I^i(\Sigma_{xy}, \Sigma_{xx}) = \tau_I^i(\Sigma_{xx}) - \tau_I^*(\Sigma_{xy})$ (d).

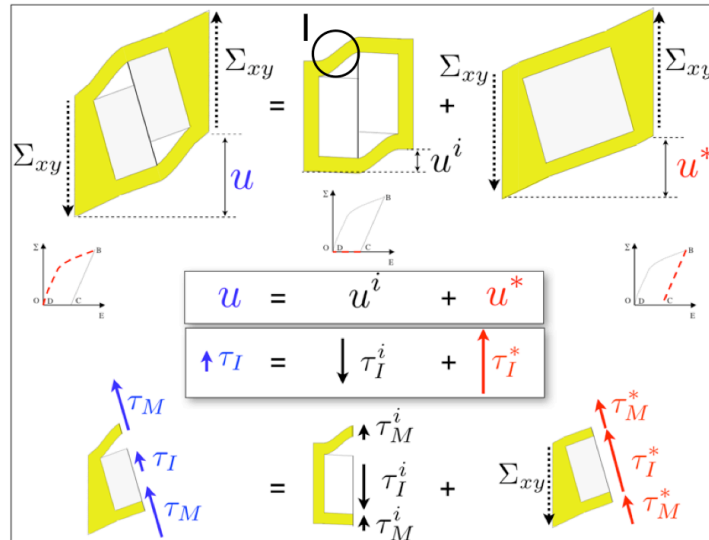


Figure 4: Confined shear on the cell: the virtual path (OC)-(CB).

The choice of the boundary conditions has to be discussed. They depend on the neighboring cell features (e.g., orientation of the transgranular crack, size of the

grain) and, more importantly, it has to account for the fact that the cell is part of an assembly. In the studied loading case and for the considered volume ratio of grains, the boundary conditions of homogeneous strain (H1 hypothesis) and homogeneous stress (H2 hypothesis) lead to different responses, H1 hypothesis being seemingly the most appropriate [6]. However, it has to be remembered that in the case of high crack density, the boundary conditions strongly fluctuate from cell to cell.

The development of the model under hypothesis H1 is now described briefly. It has to be noted that the choices for modeling are different from those that would have been made under hypothesis H2 [7]:

- **path (OC) – inelastic response**: The inelastic response is assumed to be entirely driven by the level shear of the beam 1 (see Fig. 4). The strain of the matrix is thus neglected, due to the strong stiffness contrast between the phases. As illustrated in Fig. 5-b, two cases can be distinguished. The debonded length D (Fig. 5-a) may saturate at l_x . By introducing a fictitious debond length $D_f \propto \tau_I^i$, which would be the length of a decohesion crack in a cell whose inclusion length l_x is infinite, the following cases arise

$$\begin{cases} \text{if } D_f \leq l_x \text{ then } u^i = a_1(\tau_I^i)^2 / \Sigma_{yy} \text{ and } W^i = b_1(\tau_I^i)^3 / \Sigma_{yy} \\ \text{if } D_f = l_x \text{ then we note } \tau' = \tau_I^i \\ \text{if } D_f > l_x \text{ then } D = l_x, u^i = a_1(\tau')^2 / \Sigma_{yy} + a_1(\tau_I^i - \tau') \\ \text{and } W^i = b_1(\tau')^3 / \Sigma_{yy} + b_2(\tau_I^i - \tau')^2 + b_3(\tau_I^i - \tau')\Sigma_{yy} \end{cases}$$

where $(a_i)_{i=(1,2)}$ and $(b_i)_{i=(1,2,3)}$ depend on the parameters shown in Fig. 5-a, and on the phases properties.

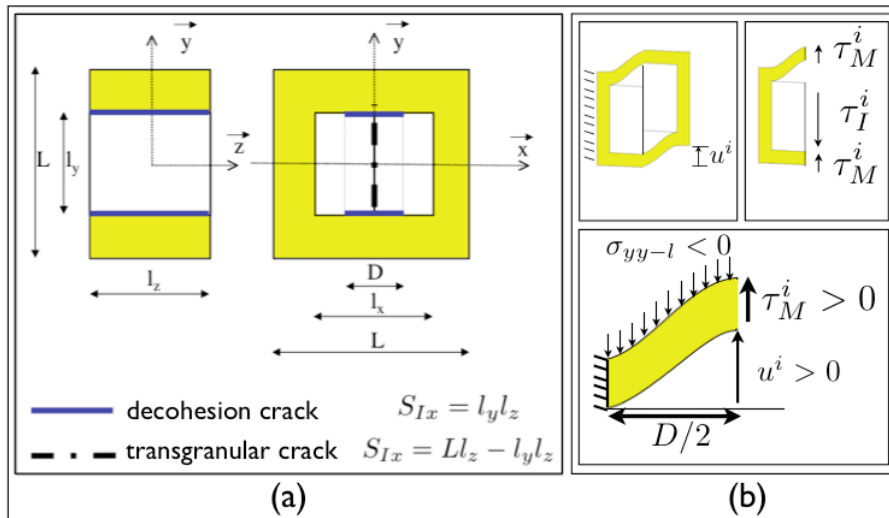


Figure 5: (a) Cell geometry. (b) Construction of the inelastic strain.

- **path (CB) – elastic response:** In the considered sliding case, the inclusion rotation needs to be taken into account during the elastic loading. The following relationships apply

$$\tau_l^* = c_2 \Sigma_{xy}, \quad u^* = a_3 \Sigma_{xy} \quad \text{and} \quad W^* = b_4 \Sigma_{xy}^2$$

and the shear stress on the crack is $\tau_l = c_1 \Sigma_{xx}$, where a_3, b_4 and $(c_i)_{i=(1,2)}$ depend on parameters shown in Fig. 5-a, and on the phases properties.

- **linking paths (OC) and (CB):** Relationship (d) allows one to express the overall strain $u/L = (u^* + u^i)/L$ and the free energy thanks to the mesoscopic loading.

Figure 6 illustrates a comparison between theoretical and numerical models, when $K_M = 1$ GPa, $K_I = 10$ GPa, $\mu_M = \mu_I = 0.3$, $L = l_z = 1$ m and $l_x = l_y = 0.79$ m.

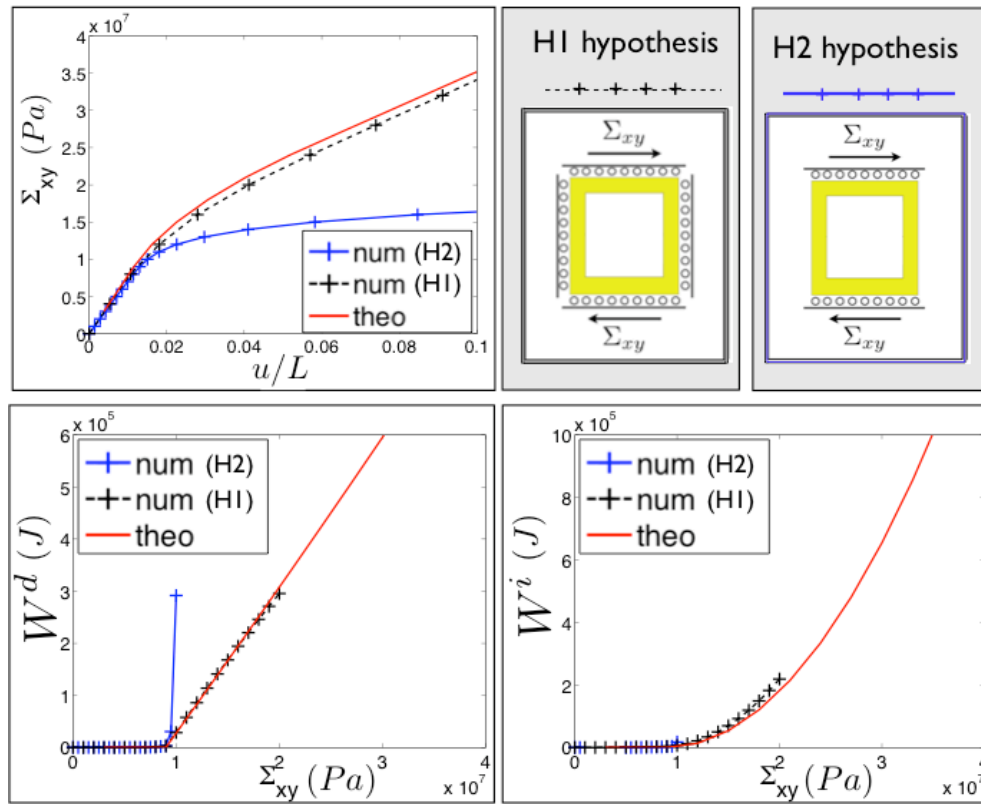


Figure 6: Comparison between numerical and theoretical responses when $\Sigma_{xx} = \Sigma_{yy} = 20$ MPa.

A good agreement between these two approaches is observed in terms of stress / strain response, dissipated energy and stored energy. It is worth noting

that the numerical response for H1 and H2 hypotheses are very different. Last, the integral Taylor-Quinney coefficient is shown in Fig. 7 for different confinement conditions. It takes values much less than unity, which means that a large amount of the external work is *stored* in the material instead of being dissipated. This result justifies the choice of the employed methodology if an accurate estimation of the dissipated energy is required.

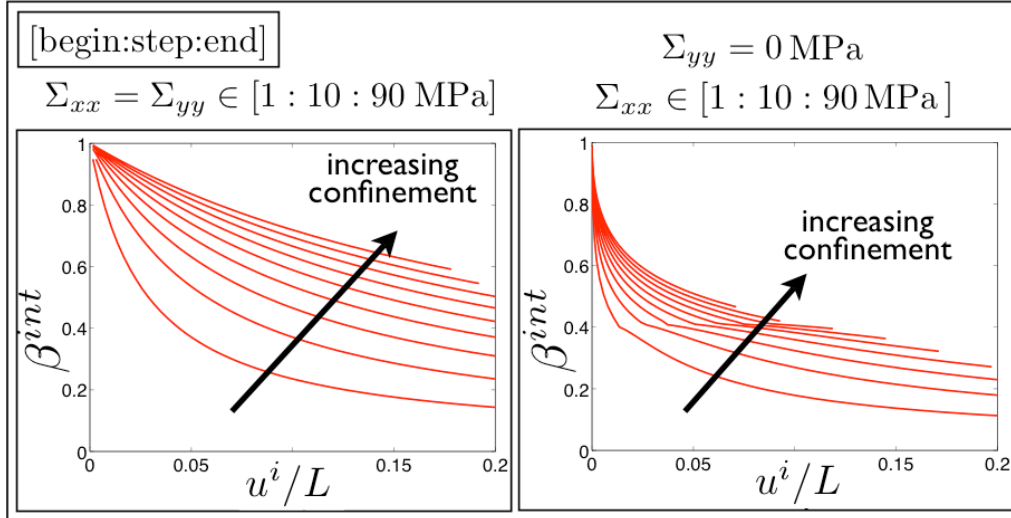


Figure 7: Integral Taylor-Quinney coefficient for different confinements.

5- Conclusion

The presented work focused on a mesoscopic analysis of a cracked cell submitted to confining stresses. It shows the usefulness of continuum thermodynamics to predict hot spots induced by friction. By showing that the stored energy is a non negligible part of the total energy of the system, it needs to be evaluated accurately to assess the dissipated energy, all the more that stored energy may be released, thus contributing to hot spot ignition, *during unloading*. It has also been shown that the choice of boundary conditions prescribed on the cell is delicate in the proposed three-scale approach. The macro-meso transition is an ongoing work.

References

- [1] F. P. Bowden, A. F. Yoffe, Initiation and growth of explosion in liquids and solids, Cambridge University Press, Cambridge, UK, 1952.
- [2] J. E. Field, N. K. Bourne, S. J. P. Palmer, S. M. Walley, Hot-spot ignition mechanisms for explosives and propellants, Phil. Trans. R. Soc. Lond. A 339 (1992) 269-283.
- [3] G. Vivier, F. Hild, M. Labrunie, P. Lambert, H. Trumel, Studying and

modelling a pressed HMX-based energetic material, in: Proc. 17th DYMAT Tech. Meeting, September 6-7/2007, Cambridge, UK.

[4] P. Lambert, Etude microstructurale d'un explosif sollicité par compression triaxiale statique, Société Sciences & Applications, report SA 06122, 2007.

[5] S. Andrieux, Y. Bamberger, J.-J. Marigo, Un modèle de matériau microfissuré pour les bétons et les roches, J. Méc. Théor. Appl. 5 (1986) 471-513.

[6] S. Zambelli, Allumage par points chauds d'un explosif comprimé soumis à l'impact d'un projectile, MSc. report, 2007.

[7] G. Vivier, H. Trumel, F. Hild, On the stored and dissipated energies in cracked systems (part 3), to be submitted.